Fungal Biology 124 (2020) 1013–1023

Contents lists available at ScienceDirect

Fungal Biology

journal homepage: www.elsevier.com/locate/funbio

Growth induced translocation effectively directs an amino acid analogue to developing zones in *Agaricus bisporus*

Koen C. Herman [a], Han A.B. Wösten [a], Mark D. Fricker [b], Robert-Jan Bleichrodt [a, *]

[a] Microbiology, Department of Biology, Utrecht University, Padualaan 8, 3584 CH, Utrecht, the Netherlands
[b] Department of Plant Sciences, University of Oxford, South Parks Road, Oxford, OX1 3RB, UK

ARTICLE INFO

Article history:
Received 15 July 2020
Received in revised form
4 September 2020
Accepted 6 September 2020
Available online 17 September 2020

Handling Editor: Dr. N.P. Money

Keywords:
Nutrient translocation
Mycelium
White button mushroom
Cords
Mushrooms

ABSTRACT

The vegetative mycelium of *Agaricus bisporus* supplies developing white button mushrooms with water and nutrients. However, it is not yet known which part of the mycelium contributes to the feeding of the mushrooms and how this depends on growth conditions. Here we used photon counting scintillation imaging to track translocation of the ^{14}C-radiolabeled metabolically inert amino acid analogue α-aminoisobutyric acid (^{14}C-AIB). Translocation to the periphery of the mycelium was observed in actively growing vegetative mycelium with a velocity of up to 6.6 mm h^{-1}, which was 30-fold higher than the growth rate. Furthermore, ^{14}C-AIB translocated to neighboring colonies after fusion by anastomosis depending on the relative growth rate in these colonies. When mushrooms started to develop, translocation of ^{14}C-AIB was redirected to the fruiting bodies via mycelium and hyphal cords. More abundant mycelial cord formation and a 5-fold higher rate of translocation was observed for cultures growing directionally from inoculum located at one side of the substrate, when compared to non-directional growth (inoculum mixed throughout the substrate). The maximum translocation distance was also greater (≥50 and 22 cm, respectively). In conclusion, ^{14}C-AIB translocation switches between vegetative growth and towards developing mushrooms, especially via cords and when source–sink relationships change.

1. Introduction

The white button mushroom *Agaricus bisporus* is a high quality food that is rich in protein and fibre and contains useful vitamins, minerals and anti-cancer polysaccharides. This fungus produces mushrooms after extensive colonisation of the substrate by a mycelial network. In the Netherlands, the substrate is typically a horse-manure-based compost. The industrial production process of this compost and subsequent growth of *A. bisporus* is characterised by four phases PI-PIV (Gerrits, 1988). In phase I (PI) thermophilic bacteria replace mesophilic bacteria, while the substrate temperature increases to 80 °C due to microbial metabolic activity. During the conditioning phase (PII) the released ammonia is sequestered by actinomycetes and thermophilic fungi, like *Scytalidium thermophilum*. Phase III (PIII) is initiated by introducing *A. bisporus* spawn to the PII compost. After 16–19 days incubation at 25 °C, the colonised PIII compost is transported to the growers, where it is topped with a layer of casing soil. This initiates phase IV (PIV), during which mushrooms are produced in 2–3 flushes at weekly intervals.

The mycelium within the compost consists of a network of hyphae that provides the growing mushrooms with food and water. However, only about half of the total carbohydrates in the compost has been consumed after mushrooms have been harvested (Chen et al., 2000; Jurak, 2015; Iiyama et al., 1994). The availability of substrate degrading enzymes does not seem to be the limiting factor (Jurak et al., 2014, 2015; Vos et al., 2017, 2018). Therefore, efficient translocation from the mycelium to the fruiting bodies may constrain overall resource utilisation.

Work in other fungi has led to the hypothesis of tip-directed bulk flow supporting long distance translocation (Jennings, 1987). This translocation would be caused by small pressure differences along the hyphae, that typically result from differential uptake of osmotically active compounds like ions and nutrients (Lew, 2005), de *novo* synthesis of osmolytes (Lew, 2011), external differential osmotic potentials (Muralidhar et al., 2016) or growth itself (Heaton et al., 2010). Bulk flow has been shown to exceed rates that would

* Corresponding author.
E-mail address: r.bleichrodt@uu.nl (R.-J. Bleichrodt).

https://doi.org/10.1016/j.funbio.2020.09.002

have been expected by diffusion alone or motor-driven movement of vesicles along the cytoskeleton. However, growth-induced bulk flow can deliver substances close to the tip, but additional mechanisms are required to cover the final distance to the apex (see Heaton et al., 2010 for a detailed explanation), such as diffusion, and cytoplasmic streaming/mixing (Bleichrodt et al., 2013; Lu et al., 2016; Pieuchot et al., 2015; Steinberg, 2014).

Many saprotrophic basidiomycetes form aggregates of individual hyphae called 'mycelial strands' (Jennings and Watkinson, 1982), 'linear organs' (Moore, 1998) or 'cords' (Tlalka et al., 2002). Cords develop predominantly on substrate with low nitrogen concentrations and high C/N ratios (Watkinson, 1975, 1979). Cords of *Serpula lacrymans* develop around vessel hyphae that become wider, thin walled, empty, and lose their septa (Helsby, 1976). Watkinson (1971, 1975) found that vessel hyphae may exude nitrogen by autolysis and stimulate aggregation of young hyphae to form strands. Branches of these hyphae do not diverge, but rather grow parallel to the vessel hyphae (Butler, 1957, 1958). This is accompanied by hyphal attachment and anastomosis (Moore, 1998), and the formation of an extracellular matrix (Jennings and Watkinson, 1982). Thick walled fibre or tendril hyphae envelope the structure, resulting in a (sub-)millimetre wide insulated cord (Mathew, 1961; Nuss et al., 1991). Some vessel hyphae may lyse and form even wider spaces in the cord. Cords have been shown to transport phosphorous (Wells et al., 1990; Wells and Boddy, 1995), nitrogen (Arnebrant et al., 1993; Tlalka et al., 2002; Watkinson, 1984), carbon (Brownlee and Jennings, 1982a,b) and water (Jennings, 1984). When cords arrive at a new food source, individual hyphae spread out from the cord and start branching to colonise the resource (Watkinson, 1971). Probably, the cue for this is the nitrogen level within the cords that holds the individual hyphae bundled together under low nutrient conditions, but when nitrogen levels in the new food source exceed the internal cord levels, the cohesive growth is lost (Moore, 1998). Connections between the newly discovered source and the original source are consolidated, radial growth from the inoculum stops and the mycelial network that is not connected to a source regresses as resources are reallocated (reviewed by Boddy, 1999). Mycelial regression is believed to be mediated by autolysis or apoptosis (Umar and Van Griensven, 1998; Watkinson, 1999).

It is not yet known which part of the mycelium contributes to the feeding of the mushrooms and how this depends on growth conditions. Therefore, we here studied resource translocation patterns during vegetative growth and mushroom development in *A. bisporus*. To this end, translocation of the ^{14}C-labeled amino acid analogue aminoisobutyric acid (^{14}C-AIB) was assessed in real time. We show that colonisation of the substrate by directional growth (one-sided inoculation) results in formation of more cords and 5-fold higher translocation rate of nutrients over a longer distance, when compared to non-directional growth (mixed inoculation of the compost). Under laboratory growth conditions this was accompanied by a higher mushroom yield. However, this was not sustained in larger, semi-industrial growth conditions.

2. Material and methods

2.1. Culturing

A. bisporus production strain A15 was routinely grown on nutrient-pour casing soil or on PII horse-manure based compost (CNC Grondstoffen BV). For network fusion experiments on casing, 80 g casing soil was manually compressed in 12 × 12 cm square Petri dishes (Greiner) and inoculated with rye grains that had been colonised with *A. bisporus* A15 (Sylvan). To test translocation following directional growth, 15 g PIII compost (12 × 3 cm) was placed next to 50 g PII compost (12 × 9 cm) in square Petri dishes (12 × 12 cm) as a 17 mm thick layer (Fig. 1A). For mushroom production, halbschalen cultures were used by tilling square dishes (Eger, 1962). To this end, 10 g PIII compost (12 × 1 cm), 40 g PII compost (12 × 8 cm) and 20 g casing soil (12 × 2 cm) were placed as blocks next to each other in dishes (similar to Fig. 1B). This resulted in directional growth. For mushroom production following non-directional growth, 50 g PIII compost in a 12 × 9 cm area was abutted by a block of 20 g casing soil (12 × 2 cm) (similar to Fig. 1C). For long-range translocation experiments, similar but larger cultures were set up in 24.5 × 24.5 cm dishes. For directional growth, 50 g PIII compost (24.5 × 3 cm), 225 g PII compost (24.5 × 13.5 cm) and 110 g casing soil (24.5 × 5.5 cm) were placed next to each other in a 25 mm thick layer (Fig. 1B). Likewise, for non-directional growth, 275 g PIII compost (24.5 × 16.5 cm) and 110 g casing soil (24.5 × 5.5 cm) were used (Fig. 1C). Cultures were incubated at 22 °C and 80% RH for about ≥30 or 14 days for these directional and non-directional growth modes, respectively, unless stated otherwise. Mushroom formation was induced by venting at 18 °C at 80% RH. To evaluate maximum translocation distance, 65 mm wide gutters of 0.5 or 1 m length were used. Gutters of 0.5 m length were filled with 45 g PIII compost, 350 g PII compost and 60 g casing soil for directional growth (Fig. 2A), or with 395 g PIII compost and 60 g casing soil for non-directional growth (Fig. 2B), at a compost density of 0.4 kg/l. Gutters of 1 m length were filled with 45 g PIII compost, 790 g PII compost and 60 g casing soil for directional growth (Fig. 2C), or with 835 g PIII compost and 60 g casing soil for non-directional growth (Fig. 2D). Generally, incubations for directional growth spanning 50 or 100 cm took over 2 or 4 months, respectively, while non-directional growth in 50 and 100 cm gutters took 1 month. ^{14}C-AIB label was applied at one end of the gutter when >10 mm mushrooms had formed on the other end (Fig. 2). Mushrooms were allowed to mature over 3 days to circa 5 cm diameter before harvesting for liquid scintillation counting (LSC).

To determine mushroom yield, 500 g PIII compost was placed at the bottom of boxes (26 x 20 × 22 cm; Manutan) and 2 kg PII compost was placed on top for directional growth (similar to Fig. 1B, but now in 3 dimensions (3D)). For non-directional growth 500 g PIII and 2 kg PII compost were mixed (similar to Fig. 1C, but now in 3D and a mix of PIII and PII compost was used, instead of only PIII compost). Alternatively, 2.5 kg PIII compost was used for non-directional growth (similar to Fig. 1C, but now in 3D). Compost was topped with 1 kg casing soil after 12, 14 and 19 days for non-directional mixed, non-directional and directional growth, respectively. Mushrooms were harvested for up to 2 months after inoculation.

2.2. Liquid scintillation counting

Cultures were labelled with 2–10 μCi 2-amino[1-^{14}]isobutyric acid (^{14}C-AIB; 2.11 GBq/mmol aqueous solution in 2% ethanol, Amersham) that was mixed with 1% Triton X-100 (Merck) in 9 g/l NaCl solution and incubated for 3 days to allow mushroom formation. Mushrooms were weighed and cut in pieces that were then dissolved in 2 ml 98% sulfuric acid (Sigma–Aldrich) per gram wet weight mushroom. This was followed by adding 9 volumes $CaCl_2$ to precipitate sulphate, which would otherwise react with the scintillation cocktail. Samples were vortexed, centrifuged for 5 min at 10,000 g, and 100 μl supernatant was transferred to a LSC tube (Pony Vial 6 ml, PerkinElmer), after which 5 ml Ultima Gold™ LSC Cocktail (Merck) was added. Samples were counted for 2 × 5 min (disintegrations per min (dpm)) using a Tri-Carb 2300 TR liquid scintillation analyser (Packard). Radioactivity was quantified using calibration curves in presence and absence of dissolved mushroom sample to correct for reduced counting efficiency in the presence of the organic material.

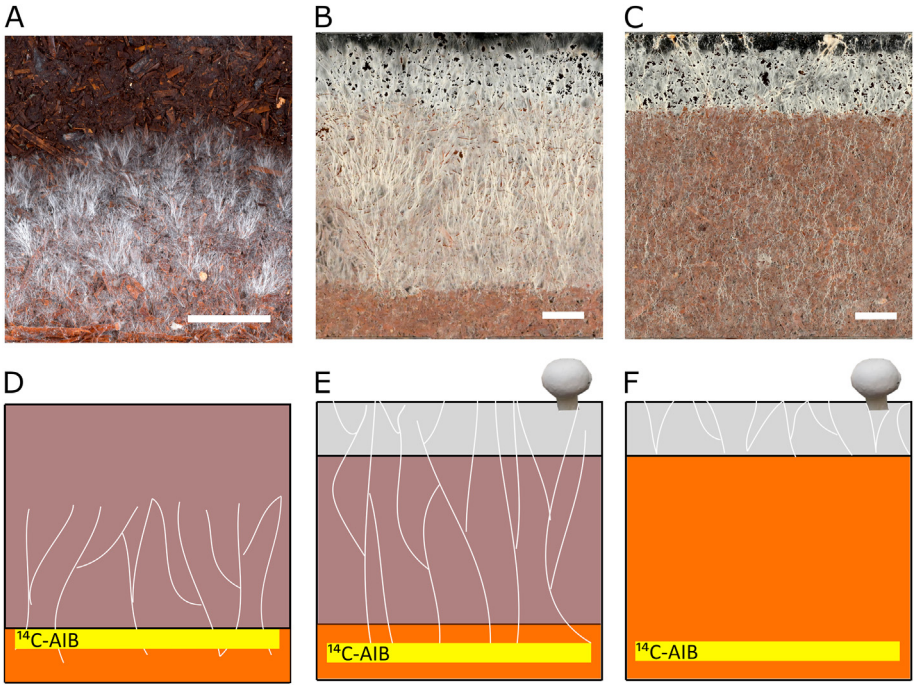

Fig. 1. Experimental set up to determine translocation efficiency of ^{14}C-AIB within directionally grown vegetative mycelium (A, D), or to mushrooms in directionally- (B, E) or non-directionally (C, F) grown halbschalen cultures. Bright field images (A–C) and schematic representations of these (D–F) are shown. The yellow rectangles indicate ^{14}C-AIB labeling zones. PIII compost (orange), PII compost (brown) and casing soil (gray) are indicated (D–F). Bars represent 3 cm (A–C). (For interpretation of the references to color/colour in this figure legend, the reader is referred to the Web version of this article.)

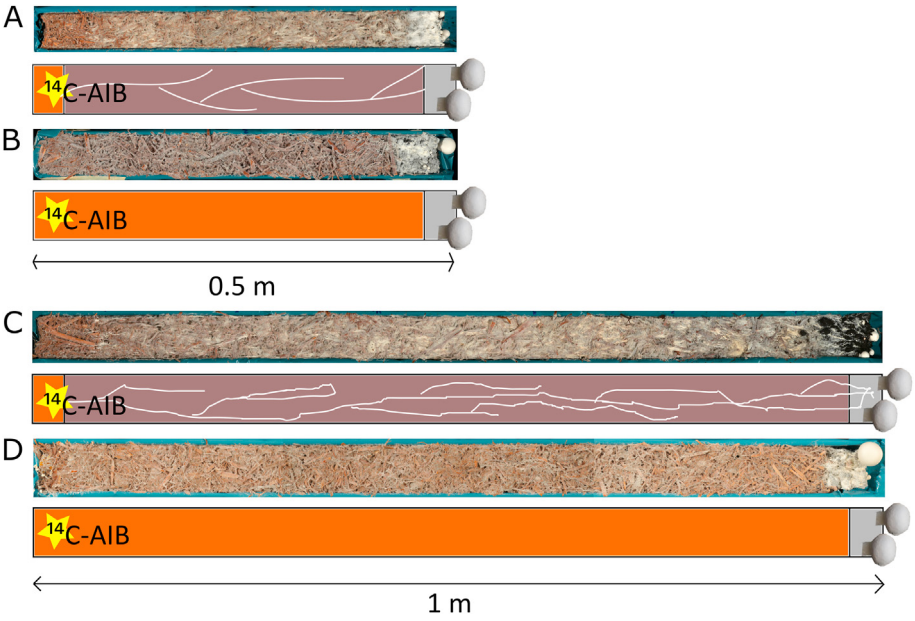

Fig. 2. Directional (A, C) and non-directional (B, D) growth in gutters of 50 cm (A, B) and 100 cm (C, D), to determine maximum translocation distance of ^{14}C-AIB to mushrooms. The yellow stars indicate the ^{14}C-AIB labelling zones. PIII compost (orange), PII compost (brown) and casing soil (gray) are indicated. Bright field images are shown at time of labelling and schematic representations thereof. After 3 days, all cultures had developed mature mushrooms (circa 5 cm in diameter). (For interpretation of the references to color/colour in this figure legend, the reader is referred to the Web version of this article.)

2.3. Statistical analysis

Means were compared using a two-tailed Student's t-test. Power was calculated using software 'PS: Power and Sample Size Calculation' version 3.1.6 (Dupont and Plummer, 1990).

2.4. Imaging ^{14}C-AIB translocation using photon counting scintillation imaging

For compost and halbschalen cultures, a 12 × 12 cm scintillation screen (Intensifying screens BioMax® Transcreen® LE, Merck) was

placed at the bottom of the Petri dish, after which PII and or PIII compost and or casing soil was added. For casing soil cultures, the screen was placed on top, covering the entire colony but with a hole cut at the position of the rye grain inoculum. The phosphorous layer of the screen was facing the substrate. 2 μCi ^{14}C-AIB was typically mixed with 2 ml 1% Triton X-100 (Merck) in 9 g/l NaCl solution and was applied to the cultures. Alternatively, pieces of Whatman® Filter Paper (Merck) were placed on the rye grain inoculum, to which 0.25–0.5 μCi undiluted label was added.

^{14}C-AIB translocation was imaged using a photon-counting system (HRPCS-3, Photek) equipped with a three-stage multi-channel plate (MCP) image intensifier that was mounted in a dark box (Tlalka et al., 2002). Signals were integrated over 1 h intervals and cultures were typically imaged for at least 72 h. Movies were imported into ImageJ, visualized using the Perceptually Uniform Colour LUT CET-D1A, and exported as AVI file with 5 frames s^{-1}. For some figures, the signal was integrated over the total time of the experiment (ImageJ summed intensity), or for intervals of several hours as indicated (using a bespoke ImageJ script, see Script S1). Translocation velocities were determined as the time for the signal to increase over background in manually defined regions of interest (ROIs), at a given distance from the inoculum. To detect accumulation of ^{14}C-AIB in mushrooms, mushrooms were longitudinally cut in half. Slices (one half was cut in longitudinal slices; the other half was cross sectioned) were put on a scintillation screen. These samples, compost and halbschalen cultures were imaged from below, while casing cultures were imaged from above, by inverting the camera system.

2.5. Modelling translocation dynamics in hyphal cords, hyphal growth and mushroom expansion

We set out to analyse flow in cords using flow mechanics by representing their hyphae as pipes. An electron microscopy image from Cairney (1990), showing a cord cross section of *Agaricus carminescens* (Fig. 3A), was used to determine the total surface area of a cord. Individual hyphae within the cord (Fig. 3B) were segmented using ImageJ, since the resolution of Fig. 3A was too low to segment individual hyphae. To this end, thresholding was performed to generate a binary image and the particle analysis tool was used to segment the hyphae and determine their cross sectional surface area. Individual hyphal radius r was calculated from the segmented cross-sectional area. Poiseuille's Law was used to calculate the pressure difference over a certain length (Pa m^{-1}) in such a pipe, required to cause the observed translocation velocity (Nobel, 1991; Brody et al., 1996), Eq. 1: $\frac{dP}{dx} = \frac{\boldsymbol{v} \cdot 8\eta}{r^2}$, where $\boldsymbol{v}$ is the velocity (m s^{-1}), η is the viscosity of the fluid (Pa·s), and r is the radius of the pipe (m). The pressure difference per hyphal length (Pa m^{-1}) was calculated based on the mean observed translocation velocity in cords of 3.5 mm h^{-1} and taking the viscosity of water (0.00089 Pa s), since this is close to the viscosity of cytoplasm (Swaminathan et al., 1997). We calculated the volume flow rate for each hypha in the segmented cord using Poiseuille's Law, Eq. 2: $Q = \frac{(P_1 - P_2)r^4}{\frac{8}{\pi}\eta L}$, where Q = volume flow rate (m^3 s^{-1}), P_1–P_2 = pressure difference (Pa) as calculated from Eq. 1, r = pipe radius (m), η = viscosity (Pa·s), L = pipe length (m) (Fig. 3B). Using the scale bars in Fig. 3A and B reproduced from Cairney (1990), we calculated the ratio of the total surface area of the cord and the part of the surface area of the cord that was represented by Fig. 3B. Total volume flow rate of the cord was then calculated by multiplying this ratio with the sum of the individual hyphae volume flow rates. This follows from that the pressure difference in parallel pipes is equal, but the sum of the flow in the individual pipes is the total volume flow rate (Engineering ToolBox, 2011). Alternatively, volume flow rates were calculated from the same pressure difference in two hypothetical scenarios: (i) a 200 μm wide cord represented as a bundle of small individual hyphae each having a 3 μm diameter (Fig. 3D); (ii) or as a bundle of 12 μm diameter vessel hyphae (Fig. 3E).

We determined how many 3 μm wide growing hyphae can be supported by a cord. To this end, the cord total volume flow rate was divided by the volume of growth per hour of a single hypha ($\pi \cdot r^2 \cdot h = \pi \cdot 1.5^2$ μm·217 μm h^{-1} (growth rate)).

The number of cords needed to support mushroom expansion was calculated as follows. Mushroom wet weight was multiplied by water content (90%) to calculate how much water it contained. This number was then divided by Q (ml h^{-1}) of a single cord of 50 cm length and by the number of hours (72 h) it took to expand the mushroom. The maximum number of mushrooms that could be formed, was calculated by dividing the total cross sectional surface area of the culture by the cross sectional surface area of the number of cords that was needed to support a single mushroom.

3. Results

3.1. ^{14}C-AIB translocates to actively growing zones of A. bisporus

Fungal hyphae consist of ~90% water and therefore growth needs a supply of water to fill the new growth volume. We assessed whether growth-induced bulk flow induces movement of water and nutrients to the growing periphery of the colony, and what the speed of that movement was using photon counting scintillation imaging (PCSI, Tlalka et al., 2002, 2007). ^{14}C-AIB was loaded at the PIII-PII compost interface after 2/3 of the surface area of the PII compost had been directionally colonised from the PIII compost (Fig. 1D). ^{14}C-AIB predominantly moved in the direction of the growing periphery and hardly within the PIII compost inoculum. The signal moved at a speed of 6.55 ± 1.38 mm h^{-1} (mean ± 95% CI) to the periphery during the first 9–15 h (Movie S1), while the growth speed was 30-fold lower (0.217 ± 0.02 mm h^{-1}). The signal became more and more intense at the periphery after this initial phase (Fig. 4E), confirming that translocation was faster than growth. The travelling signal was not homogenously spatially distributed, but was concentrated in hyphal cords, indicated by the tubular localisation of the ^{14}C-AIB signal (Fig. 4F). However, once reaching the periphery, the signal became more diffuse (Fig. 4E), indicating that the label was redistributed in finely branched hyphae. From then onwards, the translocation rate followed the growth rate (Movie S1). We hypothesised that less cord formation would decrease translocation velocity. Radially symmetric growing colonies that had been inoculated from a single rye grain spawn, produced less predominant cords (Fig. 4G). ^{14}C-AIB was loaded on the rye grain inoculum and translocated with 3.68 ± 0.31 mm h^{-1} towards the colony margin (Fig. 4G-L, Movie S2). This was about half the speed observed during directional growth. In contrast, essentially no translocation was observed when label was added to cultures that had already been fully colonised (no growth; data not shown) or that consisted of PIII compost that had been manually broken to pieces and that had been allowed to reconnect for 5 days, effectively allowing a small amount of growth everywhere (Fig. 5B).

Supplementary video related to this article can be found at https://doi.org/10.1016/j.funbio.2020.09.002

3.2. Maturing mushrooms pull ^{14}C-AIB from the compost

Mushroom expansion should generate a pull of water and nutrients from the substrate. To test this, halbschalen cultures were used to assess transport in mushroom forming cultures (Fig. 5C). Halbschalen cultures were made by placing a layer of colonised compost (PIII) adjacent to a small layer of casing soil in square Petri

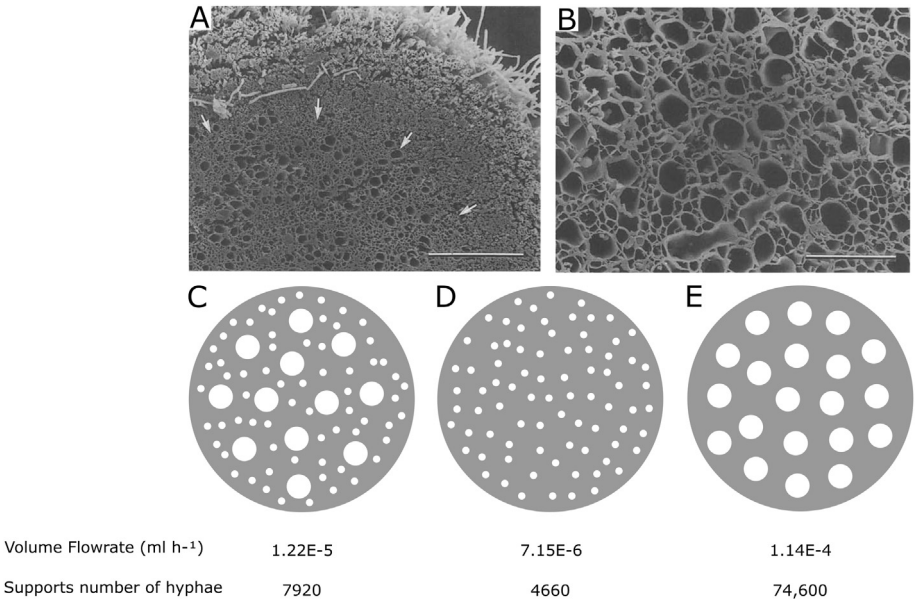

Fig. 3. Structure of cords and their volume flow rates according to three scenarios (A) Internal structure of an *A. carminescens* cord. Arrows depict the boundary of the medulla. Bar represents 20 μm (B) Magnification of the medulla showing many wide vessel hyphae. Bar represents 30 μm (C) Scenario 1 is based on the naturally observed cord (as seen in A, B) composed of both thin and vessel hyphae (D) Scenario 2 depicts a cord that is composed of only thin hyphae of Ø 3 μm (E) Scenario 3 is a cord that is exclusively composed of Ø 12 μm vessel hyphae. Volume flow rate calculations in a 5 cm long cord have been based on Poiseuille's Law (Eq. 2, Material and methods) for laminar flow in pipes, ignoring the presence of septa and taking the cytoplasmic viscosity as water. The observed translocation velocity in cords of 3.5 mm h^{-1} implies a pressure difference of 2 Pa cm^{-1} (Eq. 1). The following parameters were thus used: pressure difference 10 Pa (5 cm · 2 Pa cm^{-1}), viscosity of water (η) 8.98E-4 Pa s, cord length (L) 5 cm. Height differences, evaporation, exudation or cell wall deformation have been assumed to be zero. The cord volume flow rate and the number of hyphae at the periphery of a colony that a cord can support with the water needed for their growth is indicated for each scenario (A, B) Reprinted from 'Internal structure of mycelial cords of *Agaricus carminescens* from Heron Island, Great Barrier Reef', Vol 94/edition number 1, Cairney JWG, Pages 117–119, Copyright (1990), with permission from Elsevier. https://doi.org/10.1016/S0953-7562(09)81271-9.

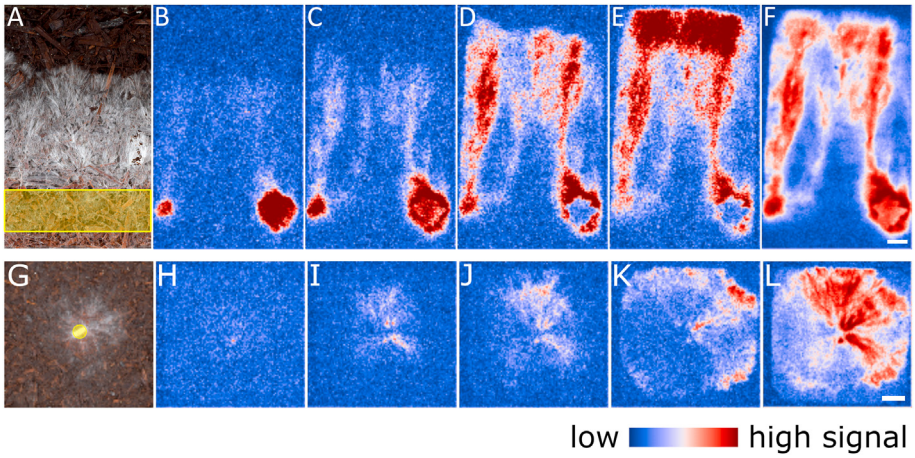

Fig. 4. ^{14}C-AIB translocation during directional (A–F) and radial colonisation (G–L) of PII compost (A, G) bright field images. Yellow regions represents labelling zones. Distribution of label after 9 or 3 h (B, H), 21 or 18 h (C, I), 42 or 36 h (D, J), and 72 h (E, K), with (F, L) representing time integration of the signal, respectively. Bars represent 1 or 2 cm (F, L), respectively. (For interpretation of the references to color/colour in this figure legend, the reader is referred to the Web version of this article.)

dishes (similar to Fig. 1F). After colonisation of the casing layer and following formation of small pins (primordia), ^{14}C-AIB was added at the far side of the compost not in contact with the casing layer. When pins did not expand during the experiment, no translocation was observed through the hyphal cords in the casing layer supporting the pins (Fig. 5D). In contrast, translocation occurred through the compost to the hyphal cords in the casing layer (Fig. 5F, Movie S3) when pins developed into mushrooms (>10 mm diameter) (Fig. 5E; the mushroom is at the upper right corner of the dish). ^{14}C-AIB was detected by PSCI throughout the mushrooms after slicing these fruiting bodies (Fig. 5G and H). A translocation velocity of 5.6 mm h^{-1} was detected from the compost into the mushroom.

Supplementary video related to this article can be found at https://doi.org/10.1016/j.funbio.2020.09.002

3.3. Directional growth promotes nutrient translocation to the mushrooms

We observed that directionally grown cultures (Fig. 1B) produced more and wider cords than non-directional growth (Fig. 1C), suggesting a better transport capacity. To test this, ^{14}C-AIB

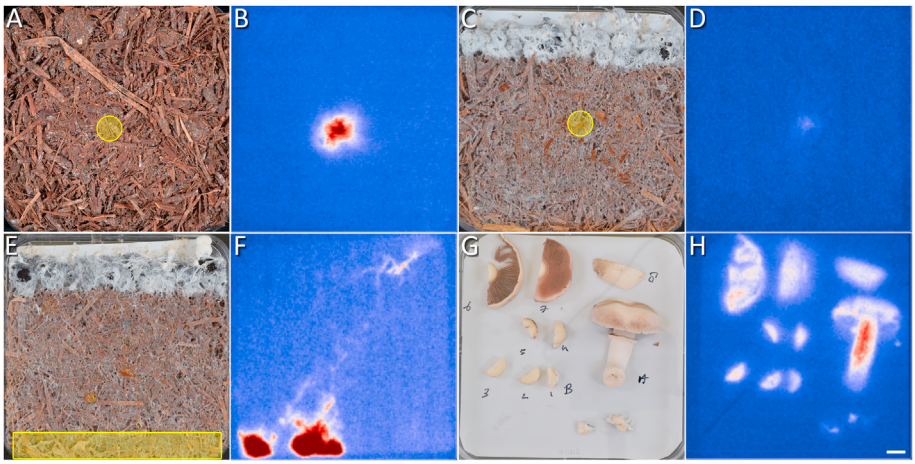

Fig. 5. Translocation of ^{14}C-AIB in cultures reconnecting the mycelial network or producing mushrooms. Bright field images (A, C, E, G), yellow regions indicate labelling zones. PCSI time integrated signal images (B, D, F, H) for 132 h (B), 84 h (D), 96 h (F) and 72 h (H). When PIII compost had been broken and allowed to regenerate for 5 days (A), no clear translocation is present (B). ^{14}C-AIB was applied to PIII compost cultures with casing soil that had either developed only small resting pins (C) or an expanding mushroom (E) (D) No translocation was observed when only resting pins are present (D), while ^{14}C-AIB translocates diagonally from the compost, through the cords in the casing soil and towards the expanding mushroom (F) (G) Mushroom harvested from culture (E), showing accumulation of ^{14}C AIB (H). Bar represents 1 cm. (For interpretation of the references to color/colour in this figure legend, the reader is referred to the Web version of this article.)

translocation to mushrooms was assessed in cultures with directional growth and non-directional growth (Fig. 1E and F, respectively). Mushrooms contained 5x times more ($p = 0.027$, power = 0.89) ^{14}C-AIB per gram in directionally growing cultures when compared to non-directionally grown cultures (347 ± 118 kdpm g^{-1} versus 70 ± 62 kdpm g^{-1}, mean ± 95% CI). We set out to test whether the enhanced transport observed for directional growth, would result in higher mushroom yield. Mushrooms were harvested from the same small-scale halbschalen cultures (Fig. 1E and F), or from larger more industrially relevant setups in boxes (similar to Fig. 1E and F but now 3-dimensional). In halbschalen cultures, directional growth gave 1.5x more yield than non-directional growth ($p = 0.027$, power = 0.9), whereas directional growth in boxes gave similar ($p = 0.63$, power = 0.06) or 1.3x lower ($p = 0.026$, power = 0.17) yields when compared to non-directional growth (PIII compost) and non-directional mixed growth (mix of PIII and PII compost at 1:4 ratio), respectively (Table 1).

Since directional growth provided better transport capacity for the mushrooms than non-directional growth, we hypothesised that directional growth might enable nutrient transport over a longer distance. To determine the maximum translocation distance for ^{14}C-AIB, gutters of 0.5 or 1 m were filled with compost and casing soil (Fig. 2). ^{14}C-AIB label was applied at one end of the gutter when >10 mm mushrooms had formed on the other end. Mushrooms were allowed to mature over 3 days. ^{14}C-AIB was detected in mushrooms harvested from 50 cm (Fig. 2A), but not 100 cm directional growth gutters (Fig. 2C), while no label was detected in mushrooms from non-directional growth (Fig. 2B and D). In the former case (Fig. 2A), the translocation speed was ≥ 6.9 mm h^{-1}.

3.4. ^{14}C-AIB translocates to neighbouring colonies growing on casing soil

The standard industrial production of mushrooms uses phase III compost that requires the formation of an interconnected network to allow transport of resources from the vegetative mycelium to developing mushrooms. To test whether fusion and cord formation enabled colony wide translocation, *A. bisporus* was grown on compressed casing soil. The colony first produced a finely branched mycelium that eventually developed into hyphal cords with diameters ranging from 76 to 382 μm (186 ± 24; mean ± 95% CI). Cords were observed extending out from the rye spawn grain. These cords branched and occasionally formed loopy lateral cross-connections. The number of cords close to the inoculum was much smaller than the number of cords at the periphery of the colony (Fig. 6A), but the diameter of the former cords was 2x larger ($p = 0.00$, power = 1.00). This suggests that cords in older parts of the colony can fuse or that more hyphae fuse with existing cords over time. The thickest cords close to the inoculum translocated most of the ^{14}C-AIB over time (Fig. 6, Movie S4); the label that had been applied to the rye grain in the centre of the colony moved outwards via these hyphal cords. The mean translocation velocity in cords on casing soil was 3.47 ± 0.03 mm h^{-1}. Less translocation was observed in a cord connected to a relatively small mycelial zone when compared to a cord that was connected to a large mycelial zone (Fig. 6B and D).

Supplementary video related to this article can be found at https://doi.org/10.1016/j.funbio.2020.09.002

Table 1
Mushroom yields for directional and non-directional (mixed) growth for three replicates.

Growth mode	Yield (mean g wet weight ± 95% CI[a])	Culture type
Directional	82 ± 5	halbschalen
Non-directional (PIII compost)	50 ± 7	halbschalen
Directional	735 ± 40	box
Non-directional (PIII compost)	766 ± 106	box
Non-directional mixed (PIII and PII compost mixed at a 1:4 ratio)	921 ± 79	box

[a] CI = confidence interval.

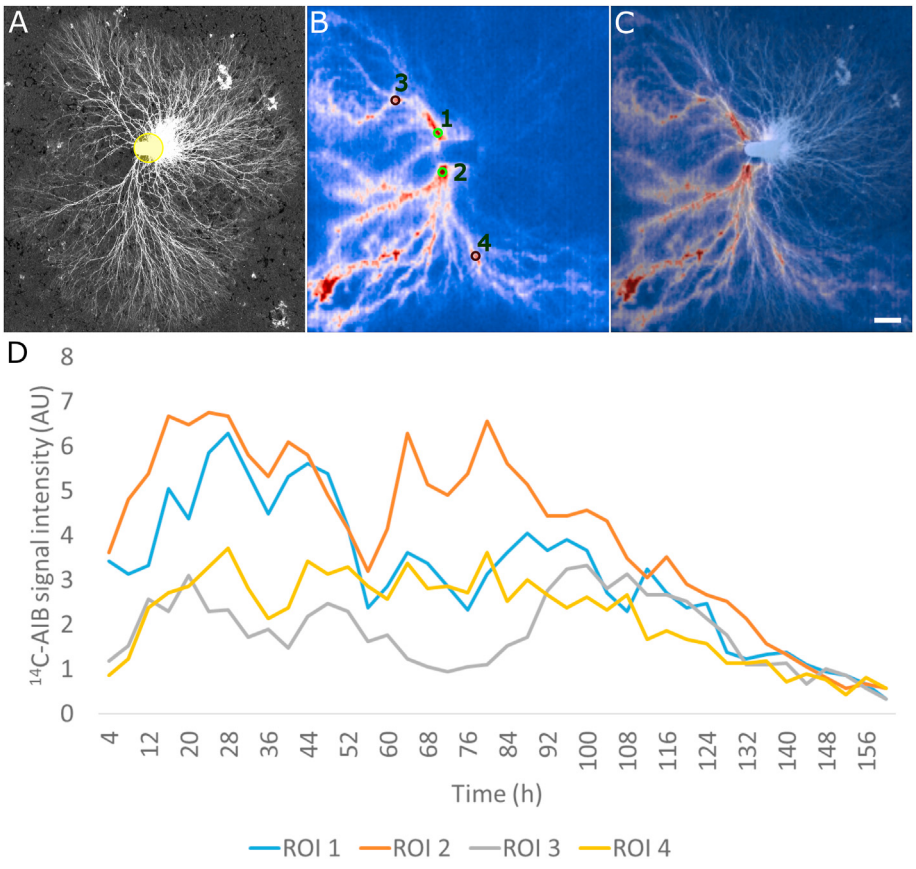

Fig. 6. Translocation of ^{14}C-AIB in a colony growing on casing soil (A) bright field image with the ^{14}C-AIB labelling zone indicated by a yellow circle (B) PCSI 4 h interval time integrated signal over 156 h (C) merge of (A) and (B). Bar represents 1 cm (D) Time-lapse intensity profile of the ^{14}C-AIB signal in regions of interest (ROI) drawn in panel (B). Accumulative signal over time was 126, 163, 73, 88 AU in the respective ROIs. (For interpretation of the references to color/colour in this figure legend, the reader is referred to the Web version of this article.)

We investigated whether neighbouring colonies could connect, thereby increasing the mycelial network from which the mushrooms could draw nutrients. When cords of neighbouring colonies met, they made functional transport connections through anastomosis as indicated by the translocation of ^{14}C-AIB between colonies through these connected cords (Fig. 7). When ^{14}C-AIB was added to the centre of one colony the label first quickly travelled to the neighbouring colony (Fig. 7B and D, Movie S5), and subsequently to the periphery in both colonies (Fig. 7B and D). When 3 colonies were grown in line and ^{14}C-AIB was added to the left one, it translocated both to the growth front, but also laterally to the neighbouring colony (Fig. 8B, Movie S6). In the second colony a similar behaviour was observed, but higher levels of the tracer accumulated at the periphery (Fig. 8B). This colony also showed most growth of all three colonies (Fig. 8A). Eventually, the furthest right colony also received some ^{14}C-AIB (Fig. 8B and D). From the image analysis it was not clear whether the middle colony received label from the left colony via the lateral cord first or via periphery interactions or both at the same time (Fig. 8D).

Supplementary video related to this article can be found at https://doi.org/10.1016/j.funbio.2020.09.002

3.5. Modelling flow in cords reveal why cords are translocation highways

We assessed the extent that cords provide enhanced transport capacity when compared to single hyphae due to their architecture. Cords in *A. bisporus* were found to have a diameter of ~200 μm. EM imaging on *A. carminescens* cords (Fig. 3A and B), which closely resemble those of *A. bisporus* (Mathew, 1961), shows that they are composed of thousands of individual hyphae (Cairney, 1990). Some of these hyphae, called vessel hyphae, have diameters of up to 14 μm. These hyphae usually have degraded septa and can thus be considered as a pipe. Poiseuille's Law can be used to calculate the pressure difference over a certain length (Pa m^{-1}) in such a pipe, required to cause an observed translocation velocity (Nobel, 1991; Brody et al., 1996; see Material and methods). We observed a translocation speed of 3.5 mm h^{-1} in cords on casing soil. In a typical 12 μm wide vessel hypha, within such a cord, this would only require a pressure difference of 2 Pa cm^{-1} (2E-5 bar cm^{-1}). For simplicity, we assumed that cytoplasm has a similar viscosity as water, that viscosity and hyphal diameter is constant throughout the network, and that hyphae do not branch or fuse. It is important to state that these assumptions may impact the modelled values.

To get an idea about the magnitude of this flow, we performed image analysis on Cairney's electron microscopy images (Cairney, 1990; see Fig. 3A and B) and segmented the cross section of each individual hypha in part of the cord. Using Poiseuille's Law for laminar flow of fluids in pipes, we calculated the volume flow rate (Q). A typical cord has a total volume flow rate of 1.22E-5 ml h^{-1} (see Fig. 3A–C). The increase in volume for an individual hypha growing (217 μm h^{-1}) in the periphery of the colony with diameter of 3 μm is 1534 μm^3 h^{-1} ($\pi \cdot r^2 \cdot h = \pi \cdot 1.5^2$ μm·217 μm h^{-1}) = 1.53E-9 ml h^{-1}. Thus a single cord, with a length of 5 cm and 200 μm in diameter, could theoretically support the growth of 7920 hyphae (1.22E-5 ml h^{-1}/1.53E-9 ml h^{-1}). Now, if we compare this to a cord

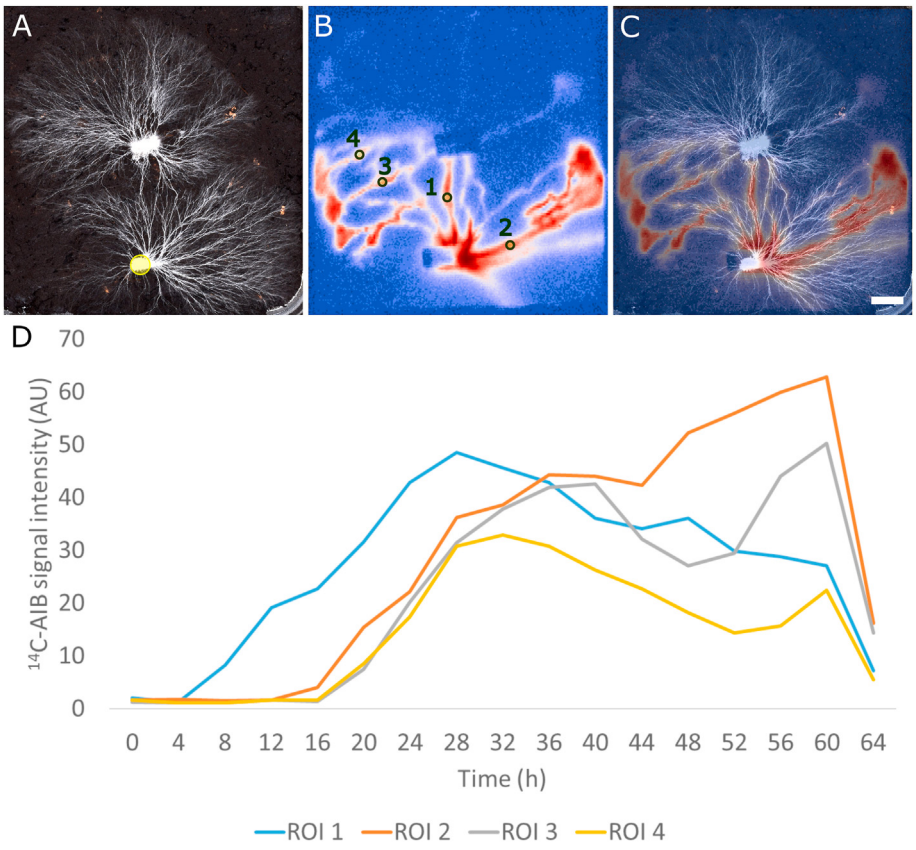

Fig. 7. Translocation of ^{14}C-AIB within and between two colonies growing on casing soil (A) Bright field image with the ^{14}C-AIB labelling zone indicated by a yellow circle (B) PCSI 4 h interval time integrated signal over 65 h. Regions with high ^{14}C-AIB intensity can be observed at the colony periphery where mycelium cannot be seen. This is explained by the presence of fine branching hyphae that explore the substrate at the colony periphery and are thus hardly visible at the resolution of the image (A) (C) merge of (A) and (B) (C) Bar represents 1 cm (D) Time-lapse intensity profile of the ^{14}C-AIB signal in regions of interest (ROI) drawn in panel (B). Accumulative signal over time was 460, 500, 385 and 252 AU in the respective ROIs. (For interpretation of the references to color/colour in this figure legend, the reader is referred to the Web version of this article.)

that would be composed of only thin hyphae of Ø 3 μm (Fig. 3D; cross section cord = $\pi \cdot r^2 = \pi \cdot 0.01^2$ = 3.14E-4 cm^2; cross section hyphae = $\pi \cdot$ 1.5E-4^2 = 7.07E-8 cm^2; thus the cord consists of 4444 thin hyphae = 3.14E-4/7.07E-8), a total volume flow rate of the cord of 7.15E-6 ml h^{-1} is obtained (4444·1.61E-9 ml h^{-1} ($Q_{single\ hypha}$)). This could only sustain growth of 4660 hyphae (7.15E-6 ml h^{-1}/1.53E-9 ml h^{-1}). On the other hand, if a cord would be exclusively composed of 278 (3.14E-4/($\pi \cdot 0.0006^2$) cm^2) Ø 12 μm vessel hyphae (Fig. 3E), a pressure difference of 2 Pa cm^{-1} would generate a volume flow rate of 1.14E-4 ml h^{-1} (278 · 4.12E-7 ml h^{-1} ($Q_{single\ hypha}$)). This would be able to support growth of 74,600 hyphae (1.14E-4 ml h^{-1}/1.53E-9 ml h^{-1}) and is a factor of ~9 more than that of a typical cord.

3.6. Mushroom formation may be limited by network capacity

We investigated whether mushroom production could be limited by the supporting network architecture using the following calculation. The water content of a typical 30 g mushroom 3 days after initiation of swelling is about 27 ml. If all the water would be taken up at the inoculum and translocated over 50 cm to the mushroom with a pressure difference of 2 Pa cm^{-1}, this would require a volume flow rate of 1.21E-5 ml h^{-1} in a single cord (Poiseuille's Law), and requires 30,865 (27 ml/1.21E-5 ml h^{-1}/72 h) typical 200 μm wide cords transporting water to the mushroom over a 72 h period. This number of cords would occupy a surface area of (π · 1E-2^2 cm · 30,865 cords) 9.7 cm^2, which is feasible within the 36 cm^2 cross section area in a gutter (see Fig. 2). This would also limit the maximum number of expanding mushrooms to 4 (36/9.7 cm^2) in such a culture, but this ignores any spacing between cords or water evaporation by the mushrooms. If we allow spacing between the cords, then less cords would be present in the culture, thus less water transport capacity would be available to supply the mushrooms. If mushrooms evaporate water, even a higher volume of water transport would be needed than just the water content of the mushrooms to replenish the evaporated water as well. Thus in both cases, the number of mushrooms that could be supplied with water would be lower. Equally, we have rarely seen more than 2 expanding mushrooms per culture, which matches these predictions.

4. Discussion

Tip directed ^{14}C-AIB translocation was only observed when vegetative cultures of *A. bisporus* were actively growing. This has also been reported for ^{14}C-glucose in *Morchella esculenta* (Amir et al., 1994), and ^{14}C-AIB in *Phanerochaete velutina* (Tlalka et al., 2002, 2003) and *S. lacrymans* (Tlalka et al., 2008a). Translocation velocities of 3.68 ± 0.31 and 3.47 ± 0.03 mm h^{-1} were observed in radially grown mycelium on compost, and cords of radially grown mycelium on casing, respectively. These rates compare with the velocity of 3.7 ± 0.4 mm h^{-1} in radially grown *P. velutina* colonies (Tlalka et al., 2008b). ^{14}C-AIB was translocated to the growing periphery at a faster rate of 6.55 ± 1.38 mm h^{-1} in directionally growing mycelium (Fig. 1D). The fact that translocation velocity in directionally grown cultures was almost two-fold higher than in

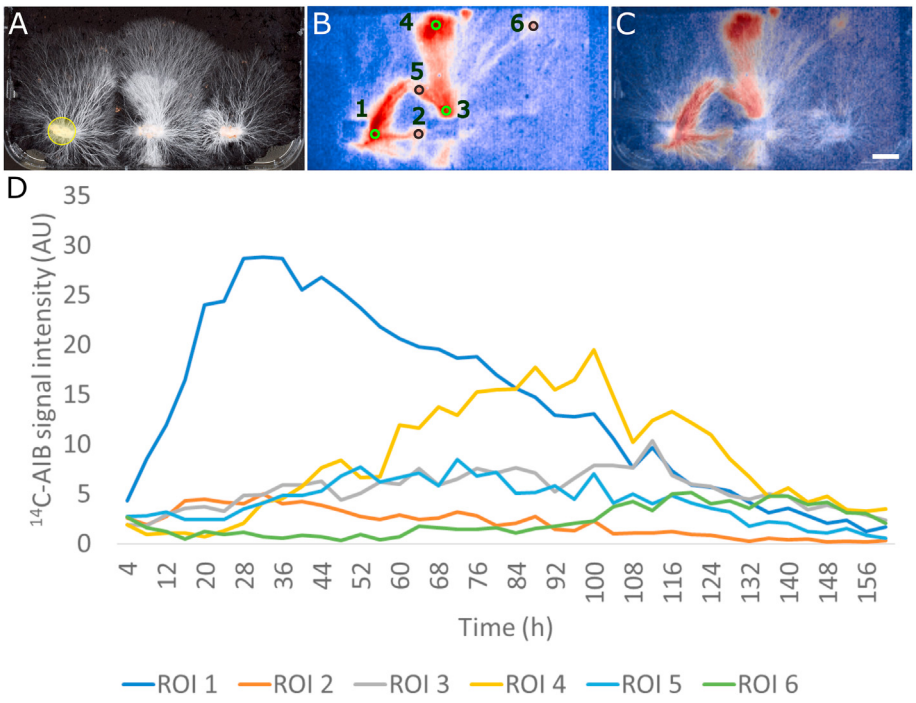

Fig. 8. Translocation of ^{14}C-AIB translocation within and between three colonies growing on casing soil (A) bright field image with the ^{14}C-AIB labelling zone indicated by a yellow circle (B) PCSI 4 h interval time integrated signal over 160 h (C) merge of (A) and (B). Bar represents 1 cm (D) Time-lapse intensity profile of the ^{14}C-AIB signal in regions of interest (ROI) drawn in panel (B). Accumulative signal over time was 556, 85, 215, 337, 169, and 90 AU in the respective ROIs. (For interpretation of the references to color/colour in this figure legend, the reader is referred to the Web version of this article.)

the other cultures, may be related to the higher level of cord formation and cords having larger diameters than in the other conditions (Fig. 1A). ^{14}C-AIB was translocated to the mushrooms with 5.6 mm/h. The maximum detectable translocation distance of ^{14}C-AIB was between 50 and 99 cm in directional (Fig. 2A and C) and 22-49 cm in non-directional growth (Fig. 1F; Fig. 2B and D). Mushrooms developed on directionally grown cultures (Fig. 1E) contained 5-fold higher levels of ^{14}C-AIB than mushrooms from non-directionally grown cultures (Fig. 1F). Together, this indicates that directional growth promotes higher transport capacity over longer distances, likely due to the presence of cords as suggested by modelling (see below).

Oscillations of ^{14}C-AIB translocation have been reported in *P. velutina* and *Coniophora puteana* (Fricker et al., 2007). We also observed temporal changes in scintillation count in *A. bisporus*, which appeared to be pulsatile with fluctuations over 30–60 h (Figs. 6D and 7D and Movie S4). However, we were not able to determine the period accurately in these relatively short time courses. Translocation was not observed after colonies had fully colonised the substrate or during regeneration of the mechanically disrupted mycelial network of PIII compost. This is in line with mathematical modelling where the extent of nutrient flow through the mycelial network was related to the amount of growth at the periphery of the colony (Heaton et al., 2010). In the case of network regeneration in PIII compost, growth occurs everywhere to enable anastomosis and reconnection, so the vectors of growth would all add up to result in a flow of zero. Together, our data indicate that long-distance translocation only occurs when there is a distinct sink, such as occurs during directional growth.

Cords in *A. bisporus* were found to have a diameter of ~200 μm. We observed a translocation speed of 3.5 mm h^{-1} in cords. In a typical 12 μm wide vessel hypha, within such a cord, this would only require a pressure difference of 2 Pa cm^{-1} (2E-5 bar cm^{-1}). This is much lower than the estimated pressure difference of 100 Pa cm^{-1} in *Neurospora crassa* hyphae of similar diameter (Lew, 2005). Since *N. crassa* hyphae do not form cords, this points to cord function. Only a fraction of the pressure difference would be needed to drive the same volume flow rate in cords in *A. bisporus* compared to single hyphae in *N. crassa*. This follows from that the pressure difference in parallel pipes is equal, but the sum of the flow in the individual pipes is the total volume flow rate (Engineering ToolBox, 2011). So, at a relatively lower differential cost of ion uptake or osmolyte accumulation, cords would be able to create a hydrostatic pressure via osmotic uptake of water and drive substantial flows to sinks located elsewhere.

We found that a typical single cord (Fig. 3C), with a length of 5 cm and 200 μm in diameter, could theoretically support the growth of ~8000 hyphae. If we compare this to a cord that would be composed of only thin hyphae of Ø 3 μm (Fig. 3D), this could only sustain growth of ~5000 hyphae, thus the presence of wide vessel hyphae is key to a cord's transport capabilities. This is further exemplified by plotting volume flow rate versus hyphal length and comparing different hyphal diameters (Fig. 9). Since this generates a hyperbole, the length of a hypha is thus far less important than its diameter for determining its volume flow rate. After only a few microns of length the asymptote is already approached, thus hyphal length has a negligible effect on translocation over distances of millimeters to centimeters. On the other hand, if a cord would be composed of only vessel hyphae (Fig. 3E), this would be able to support growth of 74,600 hyphae and is a factor of ~9 more than that of a typical cord.

^{14}C-AIB was translocated through the compost and casing layer to the developing mushrooms (Fig. 5F), but not to their earlier initials (Fig. 5D), the resting primordia (or 'pins') that did not expand. Mushrooms contain up to 50% (dry weight) mannitol (Hammond and Nichols, 1979; Rast, 1965), but only low levels of trehalose and glucose. In contrast, the vegetative mycelium contains trehalose (16%), mannitol (5%), glucose (2%) and sucrose (3%)

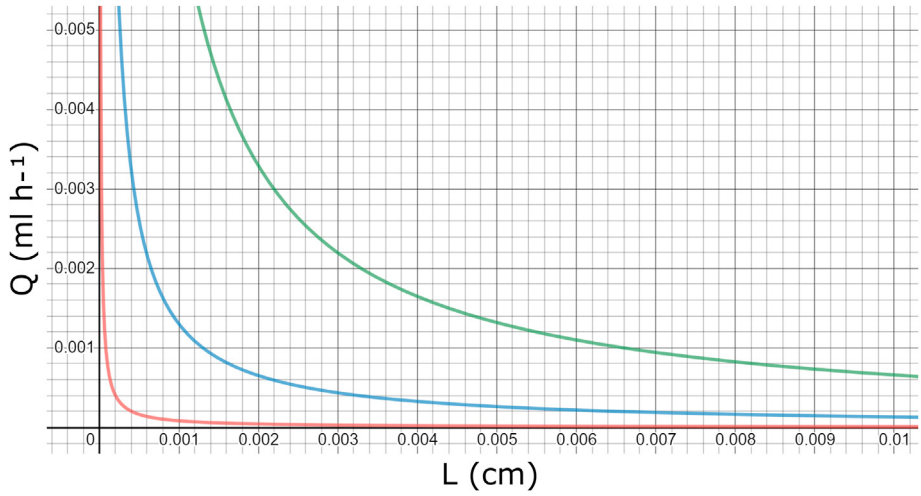

Fig. 9. The influence of hyphal length *L* and diameter on volume flow rate *Q*, taking a pressure difference of 2 Pa and diameters of 4 (red), 8 (blue) and 12 μm (green line) according to Poiseuille's Law. (For interpretation of the references to color/colour in this figure legend, the reader is referred to the Web version of this article.)

at the stage of casing the substrate (Hammond and Nichols, 1976). High mannitol levels have also been observed in mushrooms of *Lentinula edodes*, *Boletus* sp. and *Cantharellus cibarius* (Kalač, 2016; Tan and Moore, 1994). Thus, it may be that mannitol is the main osmolyte driving water translocation to mushrooms. Indeed, mannitol levels were positively correlated with yield, but for trehalose and glycogen the reverse was true (Hammond and Nichols, 1979).

Mushrooms evaporate water and even do so better than plants or human built solar steam generators (Dressaire et al., 2016; Husher et al., 1999; Xu et al., 2017). Although this goes at the expense of expansion of the mushroom, it creates a flow of water from the mycelium. This is due to the under pressure that evaporation generates and will concentrate the already present osmolytes. This is analogous with evaporation through leaves driving translocation of nutrients through xylem in plants (Siebrecht et al., 2003). This flow of water also carries new solutes to the mushrooms thereby potentially creating a positive feedback loop by building up an osmotic potential, particularly during the day when evaporation is high. This in turn could explain the quick expansion of mushrooms due to their rapid swelling and may explain why they often appear overnight, when evaporation is lower.

Together, this indicates that mushroom expansion may involve the interplay of at least five components: (i) The mycelial network should provide sufficient transport potential; (ii) the mushrooms should exploit this by maximally pulling water via osmosis, by efficiently converting trehalose and glycogen to mannitol; (iii) resources should be optimally allocated to the former two; (iv) water should be readily available in the substrate; and (v) a diurnal cycle of evapotranspiration that establishes an osmotic ratchet by drawing osmolytes into the mushroom during the day by transpiration, but with no expansion, followed by swelling at night. We found contrasting results when comparing yields in halbschalen and box cultures for directional and non-directional (mixed) growth (Table 1). Box cultures evaporated relatively much more water than halbschalen cultures did (data not shown), most likely since the latter were closed until fruiting. The fact that the improved network architecture (many wide cords) in directional growth did not give higher yield in box cultures, was thus likely due to suboptimal water availability in the compost and or casing soil, since more water would have been evaporated than in the non-directional growth cultures, due to a longer incubation time. Faster mushroom development may be obtained in the future if water availability and/or mannitol production rate could be augmented, network architecture can be optimised, or evaporation could be controlled.

Declaration of competing interest

Authors declare to have no competing interests.

Acknowledgements

This research was funded by NWO TTW grant 'Traffic control' [15493] and by a Microbiology Society research visit grant [GA000981]. The funders were not involved in study design; in the collection, analysis and interpretation of data; in the writing of the report; and in the decision to submit the article for publication.

Appendix A. Supplementary data

Supplementary data to this article can be found online at https://doi.org/10.1016/j.funbio.2020.09.002.

References

Amir, R., Levanon, D., Hadar, Y., Chet, I., 1994. The role of source-sink relationships in translocation during sclerotial formation by *Morchella esculenta*. Mycol. Res. 98, 1409–1414.

Arnebrant, K., Ek, H., Finlay, R.D., Söderström, B., 1993. Nitrogen translocation between *Alnus glutinosa* (L.) Gaertn. seedlings inoculated with *Frankia* sp. and *Pinus contorta* Doug. ex Loud seedlings connected by a common ectomycorrhizal mycelium. New Phytol. 124, 231–242.

Bleichrodt, R., Vinck, A., Krijgsheld, P., van Leeuwen, M.R., Dijksterhuis, J., Wösten, H.A.B., 2013. Cytosolic streaming in vegetative mycelium and aerial structures of *Aspergillus niger*. Stud. Mycol. 74, 3146.

Brownlee, C., Jennings, D.H., 1982a. Pathway of translocation in *Serpula lacrimans*. Trans. Br. Mycol. Soc. 79, 401–407.

Brownlee, C., Jennings, D.H., 1982b. Long distance translocation in *Serpula lacrimans*: velocity estimates and the continuous monitoring of induced perturbations. Trans. Br. Mycol. Soc. 79, 143–148.

Boddy, L., 1999. Saprotrophic cord-forming fungi: meeting the challenge of heterogeneous environments. Mycologia 91, 13–32.

Brody, J.P., Yager, P., Goldstein, R.E., Austin, R.H., 1996. Biotechnology at low Reynolds number. Biophys. J. 71, 3430–3441.

Butler, G.M., 1957. The development and behaviour of mycelial strands in *Merulius Lacrymans* (Wulf.) Fr. I. Strand development during growth from a food-base through a non-nutrient medium. Ann. Bot. 21, 523–537.

Butler, G.M., 1958. The development and behaviour of mycelial strands in *Merulius lacrymans* (Wulf.) Fr.: II. Hyphal behaviour during strand formation. Ann. Bot. 22, 219–236.

Cairney, J.W.G., 1990. Internal structure of mycelial cords of *Agaricus carminescens* from Heron Island, Great barrier Reef. Mycol. Res. 94, 117–199.
Chen, Y., Chefetz, B., Rosario, R., van Heemst, J.D.H., Romaine, P.C., Hatcher, P.G., 2000. Chemical nature and composition of compost during mushroom growth. Compost Sci. Util. 8, 347–359.
Dressaire, E., Yamada, L., Song, B., Roper, M., 2016. Mushrooms use convectively created airflows to disperse their spores. Proc. Natl. Acad. Sci. Unit. States Am. 113, 2833–2838.
Dupont, W.D., Plummer, W.D., 1990. Power and sample size calculations: a review and computer program. Contr. Clin. Trials 11, 116–128.
Eger, G., 1962. The "Halbschalentest" - a simple method for testing casing materials. MGA Bulletin 148, 159–168.
Engineering ToolBox, 2011. Pipes - in series or parallel [online] Available at: https://www.engineeringtoolbox.com/pipes-series-parallel-d_1787.html.
Fricker, M.D., Tlalka, M., Bebber, D., Takagi, S., Watkinson, S.C., Darrah, P.R., 2007. Fourier-based spatial mapping of oscillatory phenomena in fungi. Fungal Genet. Biol. 44, 1077–1084.
Gerrits, J.P.G., 1988. Nutrition and compost. In: Griensven, L.J.L.D. (Ed.), The Cultivation of Mushrooms. Darlington Mushroom Laboratories, Rustington, UK, pp. 29–72.
Hammond, J.B.W., Nichols, R., 1976. Carbohydrate metabolism in *Agaricus bisporus* (Lange) Sing.: changes in soluble carbohydrates during growth of mycelium and sporophore. J. Gen. Microbiol. 93, 309.
Hammond, J.B.W., Nichols, R., 1979. Carbohydrate metabolism in *Agaricus bisporus*: changes in non-structural carbohydrates during periodic fruiting (flushing). New Phytol. 83, 723–730.
Heaton, L.L.M., López, Maini PK., Fricker, M.D., Jones, N.S., 2010. Growth-induced mass flows in fungal networks. Proceedings of the Royal Society B 277, 3265–3274.
Helsby, L., 1976. Structural Development of Mycelium of *Serpula lacrymans*. PhD Thesis. University of Oxford.
Husher, J., Cesarov, S., Davis, C.M., Fletcher, T.S., Mbuthia, K., Richey, L., Sparks, R., Turpin, L.A., Money, N.P., 1999. Evaporative cooling of mushrooms. Mycologia 91, 351–352.
Iiyama, K., Stone, B.A., Macauley, B.J., 1994. Compositional changes in compost during composting and growth of *Agaricus bisporus*. Appl. Environ. Microbiol. 60, 1538-1546.
Jennings, D.H., 1984. Water flow through mycelia. In: Jennings, D.H., Rayner, A.D.M. (Eds.), The Ecology and Physiology of the Fungal Mycelium. Cambridge University Press, Cambridge, UK, pp. 55–79.
Jennings, D.H., 1987. Translocation of solutes in fungi. Biol. Rev. 62, 215–243.
Jennings, L., Watkinson, S.C., 1982. Structure and development of mycelial strands in *Serpula lacrimans*. Trans. Br. Mycol. Soc. 78, 465–474.
Jurak, E., Kabel, M.A., Gruppen, H., 2014. Carbohydrate composition of compost during composting and mycelium growth of *Agaricus bisporus*. Carbohydr. Polym. 101, 281-288.
Jurak, E., 2015. How Mushrooms Feed on Compost: Conversion of Carbohydrates and Lignin in Industrial Wheat Straw Based Compost Enabling the Growth of *Agaricus Bisporus*. Wageningen University, Dissertation.
Jurak, E., Punt, A.M., Arts, W., Kabel, M.A., Gruppen, H., 2015. Fate of carbohydrates and lignin during composting and mycelium growth of *Agaricus bisporus* on wheat straw based compost. PloS One 10, e0138909.
Kalač, P., 2016. Carbohydrates and dietary fiber. In: Bandeira, N., Leme, M.K., Garcia, A.C.A. (Eds.), Edible Mushrooms: Chemical Composition and Nutritional Value. Academic Press, Elsevier, USA, pp. 32–45.
Lew, R.R., 2005. Mass flow and pressure-driven hyphal extension in *Neurospora crassa*. Microbiology 151, 2685–2692.
Lew, R.R., 2011. How does a hypha grow? The biophysics of pressurized growth in fungi. Nat. Rev. Microbiol. 9, 509-518.
Lu, W., Winding, M., Lakonishok, M., Wildonger, J., Gelfand, V.I., 2016. Microtubule-microtubule sliding by kinesin-1 is essential for normal cytoplasmic streaming in *Drosophila* oocytes. Proc. Natl. Acad. Sci. Unit. States Am. 113, E4995–E5004.
Mathew, K.T., 1961. Morphogenesis of mycelial strands in the cultivated mushroom, *Agaricus bisporus*. Trans. Br. Mycol. Soc. 44, 285–290.
Moore, D., 1998. Development of form. In: Fungal Morphogenesis. Cambridge University Press, Cambridge, UK, pp. 249–287.
Muralidhar, A., Swadel, E., Spiekerman, M., Suei, S., Fraser, M., Ingerfeld, M., Tayagui, A.B., Garrill, A., 2016. A pressure gradient facilitates mass flow in the oomycete *Achlya bisexualis*. Microbiology 162, 206–213.
Nobel, P.S., 1991. Plants and fluxes. In: Physicochemical and Environmental Plant Physiology. San Diego Academic Press, San Diego, USA, pp. 508–513.
Nuss, I., Jennings, D.H., Weltkamp, C.J., 1991. Morphology of *Serpula lacrymans*. In: Jennings, D.H., Bravery, A.F. (Eds.), Serpula lacrymans: Fundamental Biology and Control Strategies. John Wiley & Sons, Chichester, UK, pp. 9–38.
Pieuchot, L., Lai, J., Loh, R.A., Leong, F.Y., Chiam, K.H., Stajich, J., Jedd, G., 2015. Cellular subcompartments through cytoplasmic streaming. Dev. Cell 34, 410–420.
Rast, D., 1965. Zur stoffwechselphysiologischen bedeutung van Mannit und Trehalose in *Agaricus bisporus*. Planta 64, 81–93.
Siebrecht, S., Herdel, K., Schurr, U., Tischner, R., 2003. Nutrient translocation in the xylem of poplar–diurnal variations and spatial distribution along the shoot axis. Planta 217, 783-793.
Steinberg, G., 2014. Endocytosis and early endosome motility in filamentous fungi. Curr. Opin. Microbiol. 20, 10–18.
Swaminathan, R., Hoang, C.P., Verkman, A.S., 1997. Photobleaching recovery and anisotropy decay of green fluorescent protein GFP-S65T in solution and cells: cytoplasmic viscosity probed by green fluorescent protein translational and rotational diffusion. Biophys. J. 72, 1900–1907.
Tan, Y.H., Moore, D., 1994. High concentrations of mannitol in the shiitake mushroom *Lentinula edodes*. Microbios 79, 31-35.
Tlalka, M., Watkinson, S.C., Darrah, P.R., Fricker, M.D., 2002. Continuous imaging of amino-acid translocation in intact mycelia of *Phanerochaete velutina* reveals rapid, pulsatile fluxes. New Phytol. 153, 173–184.
Tlalka, M., Hensman, D., Darrah, P.R., Watkinson, S.C., Fricker, M.D., 2003. Non-circadian oscillations in amino acid transport have complementary profiles in assimilatory and foraging hyphae of *Phanerochaete velutina*. New Phytol. 158, 325–335.
Tlalka, M., Bebber, D.P., Darrah, P.R., Watkinson, S.C., Fricker, M.D., 2007. Emergence of self-organised oscillatory domains in fungal mycelia. Fungal Genet. Biol. 44, 1085–1095.
Tlalka, M., Fricker, M., Watkinson, S., 2008a. Imaging of long-distance alpha-aminoisobutyric acid translocation dynamics during resource capture by *Serpula lacrymans*. Appl. Environ. Microbiol. 74, 2700-2708.
Tlalka, M., Bebber, D.P., Darrah, P.R., Watkinson, S.C., Fricker, M.D., 2008b. Quantifying dynamic resource allocation illuminates foraging strategy in *Phanerochaete velutina*. Fungal Genet. Biol. 45, 1111-1121.
Umar, M.H., Van Griensven, L.J.L.D., 1998. The role of morphogenetic cell death in the histogenesis of the mycelial cord of *Agaricus bisporus* and in the development of macrofungi. Mycol. Res. 102, 719–735.
Vos, A.M., Jurak, E., Pelkmans, J.F., Herman, K., Pels, G., Baars, J.J., Hendrix, E., Kabel, M.A., Lugones, L.G., Wösten, H.A.B., 2017. H_2O_2 as a candidate bottleneck for MnP activity during cultivation of *Agaricus bisporus* in compost. Amb. Express 7, 124.
Vos, A.M., Jurak, E., de Gijsel, P., Ohm, R.A., Henrissat, B., Lugones, L.G., Kabel, M.A., Wösten, H.A.B., 2018. Production of α-1,3-L-arabinofuranosidase active on substituted xylan does not improve compost degradation by *Agaricus bisporus*. PloS One 13, e0201090.
Watkinson, S.C., 1971. The mechanism of mycelial strand induction in *Serpula lacrimans*: a possible effect of nutrient distribution. New Phytol. 70, 1079–1088.
Watkinson, S.C., 1975. The relation between nitrogen nutrition and formation of mycelial strands in *Serpula lacrimans*. Trans. Br. Mycol. Soc. 64, 195–200.
Watkinson, S.C., 1979. Growth of rhizomorphs, mycelial strands, coremia and sclerotia. In: Burnett, J.H., Trinci, A.P.J. (Eds.), Fungal Walls and Hyphal Growth. Cambridge University Press, Cambridge, UK, pp. 93–113.
Watkinson, S.C., 1984. Morphogenesis of *Serpula lacrimans* colony in relation to its function in nature. In: Jennings, D.H., Rayner, A.D.M. (Eds.), Ecology and Physiology of the Fungal Mycelium. British Mycological Society Symposium. Cambrdige University Press, Cambridge, UK, pp. 165–184.
Watkinson, S.C., 1999. Metabolism and hyphal differentiation in large basidiomycete colonies. In: Gow, N.A.R., Robson, G., Gadd, G.M. (Eds.), The Fungal Colony. Cambridge University Press, Cambridge, UK, pp. 127–157.
Wells, J.M., Hughes, C., Boddy, L., 1990. The fate of soil-derived phosphorus in mycelial cord systems of *Phanerochaete velutina* and *Phallus impudicus*. New Phytol. 114, 595–606.
Wells, J.M., Boddy, L., 1995. Phosphorus translocation by saprotrophic basidiomycete mycelial cord systems on the floor of a mixed deciduous woodland. Mycol. Res. 99, 977–980.
Xu, N., Hu, X., Xu, W., Li, X., Zhou, L., Zhu, S., Zhu, J., 2017. Mushrooms as efficient solar steam-generation devices. Adv. Mater. 29, 1606762.